

## **Gas flow traceability for non-conventional and renewable gases**

**Dr. Jos van der Grinten, Physikalisch-Technische Bundesanstalt (PTB)**

**Dr. Bodo Mickan, Physikalisch-Technische Bundesanstalt (PTB)**

**Dr. Henk Riezebos, DNV Netherlands B.V.**

**Dr. Dennis van Putten, DNV Netherlands B.V.**

---

### **1 INTRODUCTION**

DNV in Groningen, Netherlands has initiated a Joint Industry Project (JIP) [1] to study the performance of currently available metering technologies when operating non-conventional gases. These gases can contain high-CO<sub>2</sub> percentages from biogases or related to carbon capture and storage (CCS). Also, hydrogen can be mixed into natural gases in the gas grids as part of the energy transition. The objective of the study is to understand instrument sensitivity for these gases and to define scaling rules which allow meters to be calibrated on gases different from the field application.

For the JIP experiments four turbine gasmeters and nine ultrasonic gasmeters of several manufacturers are tested with different gases. A traceable reference system is needed with proven uncertainty related to type of gas or the composition of the gas mixture.

For this reason, a set of references was designed and built. First a flow reference system to cover all reference flows within the specified conditions of the Multi-Phase Flow facility of DNV (minimum gas flow 16 m<sup>3</sup>/h and maximum gas flow 1000 m<sup>3</sup>/h) consisting of two lines equipped with Coriolis meter and turbine gas meters. To provide better overall uncertainty at specific flowrates the reference system was extended with a set of five Critical Flow Venturi Nozzles (CFVNs). For CFVNs a procedure is available that allows scaling of the nozzle performance to any type of gas and any pressure [3]. The model used, has only one free parameter that can be obtained by an air flow calibration. For the turbine gasmeters PTB developed a model [4],[5] that allows scaling in the Reynolds domain, taking into account friction forces, meter bearing and the pressure and temperature difference between the pressure measurement point on the turbine gasmeter and the thermowell behind the meter. For Coriolis meters the claim is that the meter operates independent of the type of gas. However, for real accurate measurements corrections need to be made [7],[8],[9].

The objective of this paper is to show how, with the present knowledge, an accurate and stable reference system can be constructed, that operates independently of pressure and the type of gas or the gas composition. The performance of the meters under test is discussed in a second paper [2].

## 2 EXPERIMENTAL SET-UP AND MEASUREMENT PROGRAMME

### 2.1 Test facility for all gases at DNV in Groningen

Since 2013 DNV operates the Multi-Phase Flow facility, which is schematically displayed in Fig. 1. The facility is a loop in which on the right-hand side the oil, water and gas flows are mixed, sent through the flow test section, pumped, and separated. For gas there is an additional return line, used when no gas is needed in the test section. By pumping around liquids, a considerable pressure drop up to 25 bar can be achieved, even when only gas is pumped.

This possibility is exploited in the current JIP. The twin screw pump, having its own oil circuit, can now be used to pump gas. The oil water separator, and the oil and water circuits are switched off. The knock-out and the cyclones are used to remove any remnants of the heavy oil from the pump. The test line at the bottom of Fig. 1 is the location of the meters under test and the flow references. The gas flow characteristics are listed in Table 1. The loop is flexible with respect to the gases or gas mixtures to be used.

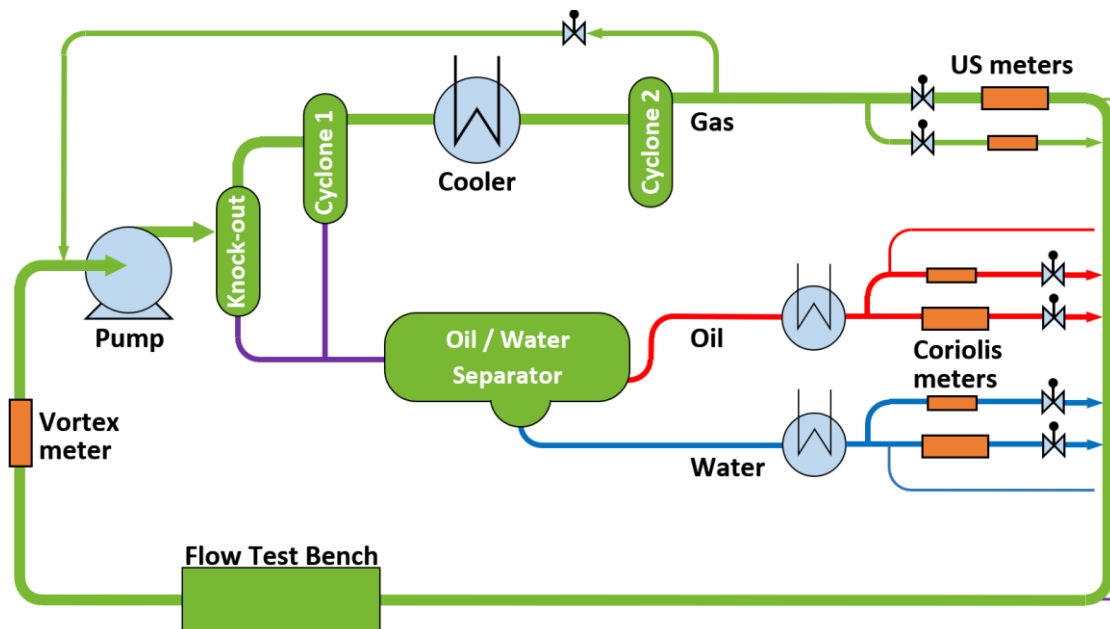


Fig. 1 – Simplified process flow diagram of the DNV Multi-Phase Flow loop Groningen. The flow test bench section is where meters under test and flow references are installed.

**Table 1 – Gas loop specifications**

Property	Range
Actual flow range	10 – 1000 m <sup>3</sup> /h
Temperature range	5 – 35 °C
Absolute pressure range	6 – 34 bar
Pressure drop over test section	0 – 25 bar
Gas	Groningen gas (G-gas), G-gas mixtures Pure gases: CH <sub>4</sub> , CO <sub>2</sub> , N <sub>2</sub> , Ar, ...

## 2.2 Reference system design

The flow reference system is installed in the gas loop of the multi-phase facility, downstream of the meters under test. It consists of two lines DN150 and DN100, each equipped with a Coriolis mass flow meter and a turbine gasmeter, followed by five parallel lines with critical flow Venturi nozzles and a DN150 bypass. Between the Coriolis and the turbine gasmeters is 10D straight length. The set-up is schematically displayed in Fig. 2. The instrument characteristics and operating range at actual conditions are listed in Table 2.

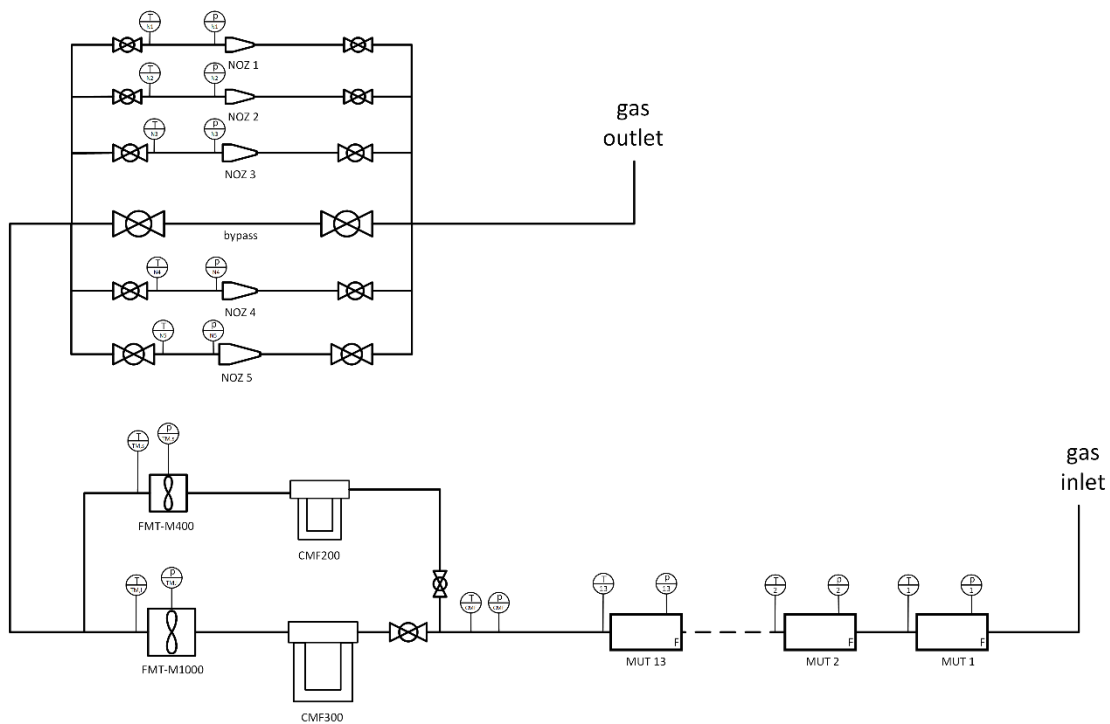


Fig. 2 – Test set-up schematic. From the right, the gas flows first through the meters under test, then through the reference Coriolis meters, the reference turbine meters, and the reference Critical Flow Venturi Nozzles.

**Table 2 – Characteristics of reference instrumentation. For the nozzles the throat diameter is shown, for the other instruments this is the nominal connection diameter. The rated nozzle flows are based on Groningen gas and are independent of pressure.**

ID	Instrument	Type	Diameter / mm	Manufacturer	Range at actual conditions
N1	sonic nozzle	toroidal	D5	Ehrler	16.5 m <sup>3</sup> /h
N2	sonic nozzle	toroidal	D8	Ehrler	41.5 m <sup>3</sup> /h
N3	sonic nozzle	toroidal	D12	Ehrler	100 m <sup>3</sup> /h
N4	sonic nozzle	toroidal	D20	Ehrler	275 m <sup>3</sup> /h
N5	sonic nozzle	toroidal	D27	Ehrler	510 m <sup>3</sup> /h
TM6	turbine meter	FMT-M400	DN100	FMG	40 - 400 m <sup>3</sup> /h
TM7	turbine meter	FMT-M1000	DN150	FMG	100 - 1000 m <sup>3</sup> /h
CMF8	Coriolis meter	CMF 200	DN100	Emerson	4355 - 43550 kg/h
CMF9	Coriolis meter	CMF 300	DN150	Emerson	13608 - 136080 kg/h

The gas flow is sampled every 3.5 minutes by a process gas chromatograph (PGC). The sample point is located before the first meter under test. The GC is validated

daily after the test with a gas mixture containing all gas components relevant for the JIP. The obtained calibration factors were applied to the composition measurements, which generally lead to composition uncertainties of 0.1 mol% maximum. After the execution of the test, the composition was further optimised by using the measured speed of sound of multiple ultrasonic flow meters and comparing these measured values with the theoretical AGA10 [10] values based on pressure, temperature and composition. Small adjustments of the composition, within the PGC uncertainty of 0.1 mol%, were performed to achieve the most consistent speed of sound measurements.

### 2.3 Test conditions as part of JIP test program

The experiments are performed with nitrogen, methane, Groningen gas and mixtures of G-gas with up to 30 mol% hydrogen and G-gas with up to 20 mol% carbon dioxide. The test pressures are 16 and 32 bar absolute. Table 3 gives an overview of the test programme as conducted in the period of 20 January till 10 February 2021.

**Table 3 – JIP test programme as performed in the period of 20 January till 10 February 2021. In total 10 different test gases are used.**

Test day	Gas composition [mol%]		Pressure [bar]
1	N <sub>2</sub>		16
2	N <sub>2</sub>		32
3	CH <sub>4</sub>		16   32
4	G-gas		16   32
5	G-gas + 5% H <sub>2</sub>	G-gas + 10% H <sub>2</sub>	32
6	G-gas + 15% H <sub>2</sub>	G-gas + 20% H <sub>2</sub>	32
7	G-gas + 5% H <sub>2</sub> , G-gas + 10% H <sub>2</sub>	G-gas + 15% H <sub>2</sub> (5 points)	16
8	G-gas + 20% H <sub>2</sub>	G-gas + 30% H <sub>2</sub> (full matrix)	16
9	G-gas (7 reference points)	G-gas + 10% CO <sub>2</sub>	16
10	G-gas + 20% CO <sub>2</sub>	G-gas + 10% CO <sub>2</sub>	16   32
11	G-gas + 20% CO <sub>2</sub>	G-gas + 10% CO <sub>2</sub>	32

## 3 PRE-CALIBRATION OF REFERENCES

### 3.1 Nozzles

For the project five toroidal-throat CFVNs were manufactured according to ISO 9300 [6]. The nozzles are characterized by their nominal throat diameters in mm: D5, D8, D12, D20 and D27, which correspond to the nominal flowrates of 16, 40, 100, 250 and 500 m<sup>3</sup>/h, respectively.

The sonic nozzles were calibrated as described in [3]. Initially, all nozzles were geometrically calibrated to establish compliance with the ISO 9300 standard [6]. Fig. 3 displays the non-dimensional nozzle radius  $r/d_{throat}$  versus the non-dimensional position  $z/d_{throat}$ . Negative values refer to the position upstream of the nozzle throat  $z/d_{throat} = 0$ .

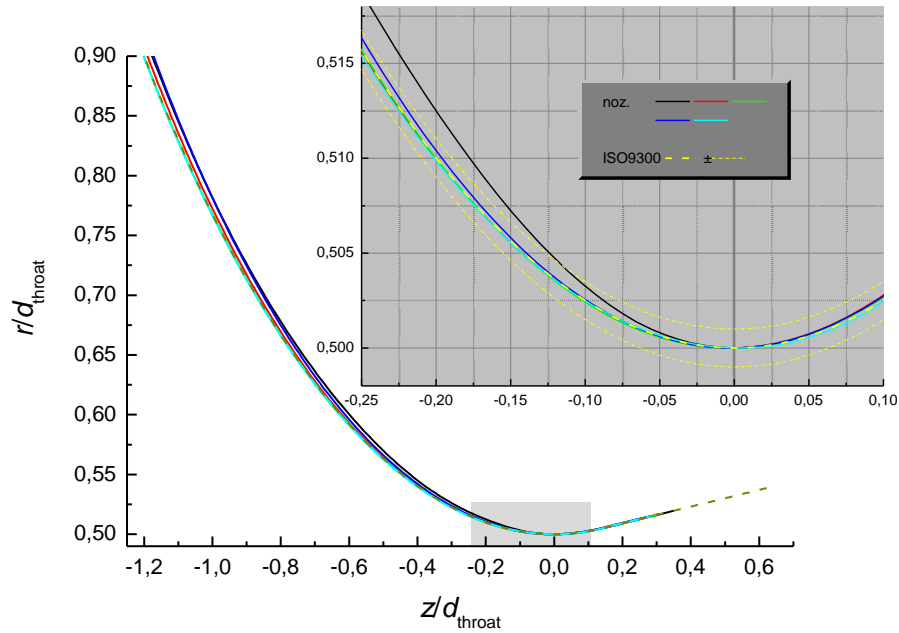


Fig. 3 – Calibration result of the five sonic nozzles (CFVNs). The non-dimensional nozzle radius  $r/d_{throat}$  is displayed as a function of the non-dimensional position  $z/d_{throat}$  in the nozzle, where  $z = 0$  corresponds to the nozzle throat. Negative  $z$  values refer to the upstream part of the nozzle. The line colours correspond to the nozzle as follows: D5 black, D8 red, D12 green, D20 dark blue and D27 cyan. The ISO 9300 curve and its tolerances are marked in yellow. The graph with the grey background is an enlargement of the grey part of the main graph.

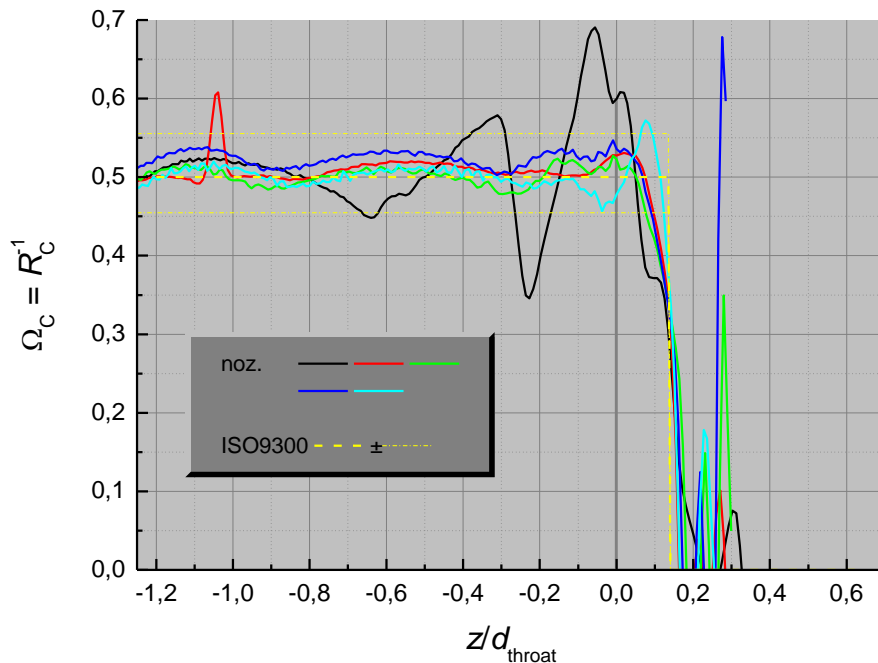


Fig. 4 – Calibration result of the five sonic nozzles (CFVNs). The curvature  $\Omega_c = R_c^{-1}$  is displayed as a function of the non-dimensional position  $z/d_{throat}$  in the nozzle, where  $z = 0$  corresponds to the nozzle throat. Negative  $z$  values refer to the upstream part of the nozzle. The line colours correspond to the nozzle as follows: D5 black, D8 red, D12 green, D20 dark blue and D27 cyan. The ISO 9300 curve and its tolerances are marked in yellow.

The nozzle curvature  $\Omega_C$  is calculated from

$$\Omega_C = \frac{1}{R_C} = \frac{r_n''}{(1 + r_n'^2)^{1.5}} \quad \text{with} \quad r_n = \frac{r}{d_{throat}} \quad (1)$$

where  $r_n'$  and  $r_n''$  denote the first and second derivatives of  $r_n$  with respect to  $z/d_{throat}$ . The result is shown in Fig. 4. Except for the smallest nozzle D5, all nozzles match the tolerances. This result is much better than the results of two different nozzles shown last year [3].

The next step is that all five nozzles are flow calibrated with atmospheric air at PTB. The result is shown in the top-left graph of Fig. 5. The five data points correspond to each of the nozzles. The dashed lines represent the curves of the analytic interpolation and the solid lines represent the result based on the numerical solution of the boundary-layer equations. The details of this procedure are fully explained in a previous paper [3]. All ten lines are within the measurement uncertainty of each of the data. Please note that the difference between the top line and the bottom line is 0,1% maximum, which allows all nozzles to be represented by a single curve shown in the top-right graph of Fig. 5.

In order to verify the  $C_D$  factor in the upper Reynolds range, three nozzles were

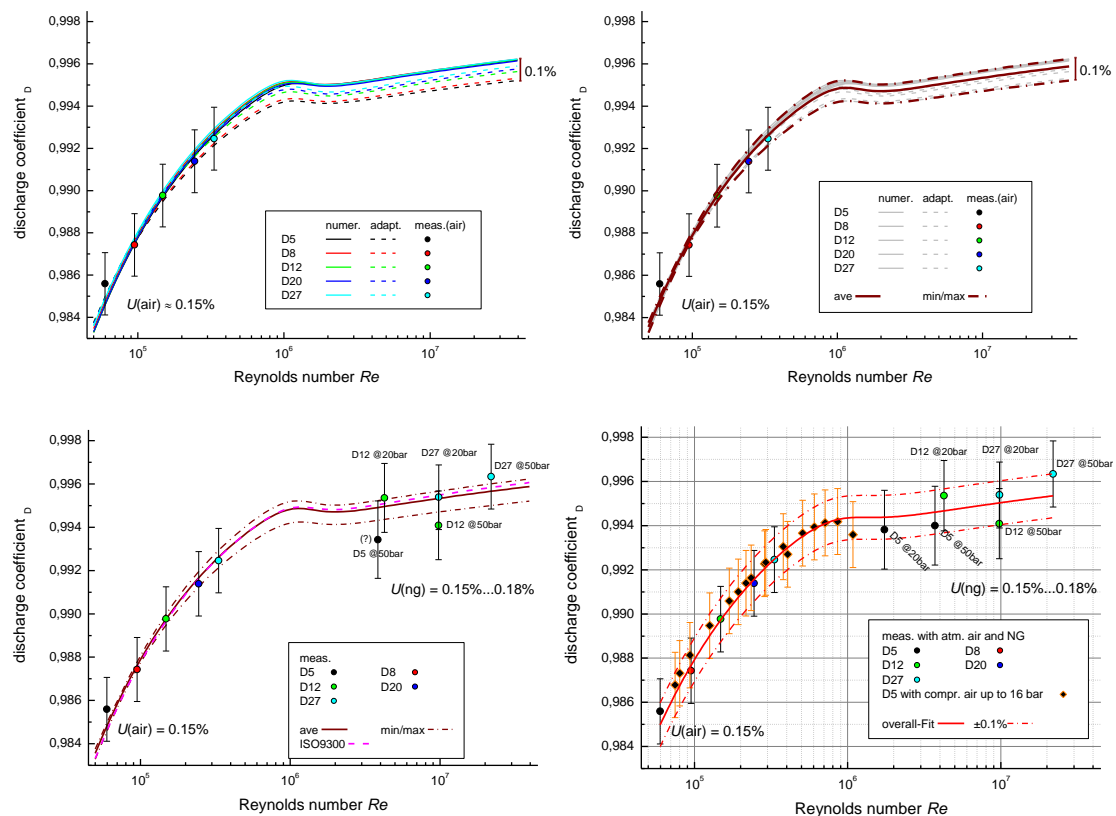


Fig. 5 – Results of the sonic nozzle calibrations. The  $C_d$  factor is plotted a function of the nozzle throat Reynolds number  $Re$ . Top left: measurements and predicted curves based on atmospheric air measurements. Top right: average curve (thicker lines) based on all ten predictions. Bottom left: additional checks with 20 bar and 50 bar natural gas. Bottom right: additional checks of the D5 nozzle using compressed air. The solid curve is identical to the curve in the top-right figure. The expanded uncertainty is 0.10%.

also calibrated at pigsar at pressures of 20 bar and 50 bar. The results are displayed in the bottom-left graph of Fig. 5. The  $C_d$  factor of D5 at 20 bar and 50 bar and the  $C_D$  factor of D12 at 50 bar are outside the predicted range. For that reason, an additional calibration of the D5 nozzle was performed at the 16-bar air test rig of PTB. In this facility the upstream pressure of the sonic nozzle can be varied between 16 bar and the lowest pressure at which the nozzle flow is still critical. The result is shown in the bottom-right graph of Fig. 5. The additional data follow the predicted curve well and by enlarging the uncertainty of the predictive function all data fit. This brings the overall uncertainty of the nozzle curves to 0.10%.

### 3.2 Coriolis meters

The Coriolis reference system consists of two Emerson Micromotion CMFs: a CMF200 in the 4" line and a CMF300 in the 6" line. The meters provide the mass flow directly and were calibrated at the ISO17025-accredited water calibration laboratory of Emerson in Ede. These calibrations were carried out at slightly over 2 bar absolute pressure and showed mass flow deviations of less than 0.02% with an expanded uncertainty of 0.02%. For the application of both Coriolis meters to high-pressure gas conditions of the JIP, the meters require a compensation for the operating pressure and the compressibility. This compensation can be written as

$$q_{g,CMF}^c = q_{g,CMF} \cdot f_p \cdot f_c, \quad (2)$$

where  $f_p$  is the pressure compensation factor and  $f_c$  the compressibility compensation factor.

The pressure compensation is based on the knowledge of the vendor and the pressure compensation factors are given in [8]

$$f_p = \frac{1}{1 + a_p(p - p_c)} \quad (3)$$

where  $p_c$  is the calibration pressure (2 bara) and  $a_p$  is a meter specific coefficient. For the CMF200 this parameter  $a_p = -0.009\%/bar$  and for the CMF300  $a_p = -0.008\%/bar$ . It is noted that also the density output from the CMFs can also be compensated for pressure, however, this meter output is not used in the reference system directly and only used for verification purposes.

The compressibility correction is based on a theoretical model developed in [9] and requires the angular tube frequency  $\omega$ , the tube radius  $r$ , and the speed of sound  $c$ , as an input. The compressibility compensation is then given by:

$$f_c = \frac{1}{1 + a_c \frac{1}{2} \left( \frac{\omega}{c} r \right)^2} \quad (4)$$

The parameter  $a_c$  is an experience factor developed by the vendor and is typically of the order 1.

To verify the CMFs, both meters were installed in the ISO17025-accredited test facility of DNV in Groningen and tested at 9, 16 and 32 bar under natural gas conditions. These results were not used to adjust the meter factor. Due to space constraints the small CMF required a diagonal installation in the DNV test facility to decrease the height of the reference measurement skid. This installation induced additional torque on the CMF200 meter body and therefore the results could not be

used for the check of the water calibration. After this experience the skid was modified to allow horizontal installation of the CMF200. The installation of the large CMF300 was not altered and the results of the verification runs are presented in Fig. 6 for the three pressures, where the error bars indicate the expanded uncertainty ( $k = 2$ ) of the combined facility CMC and meter repeatability.

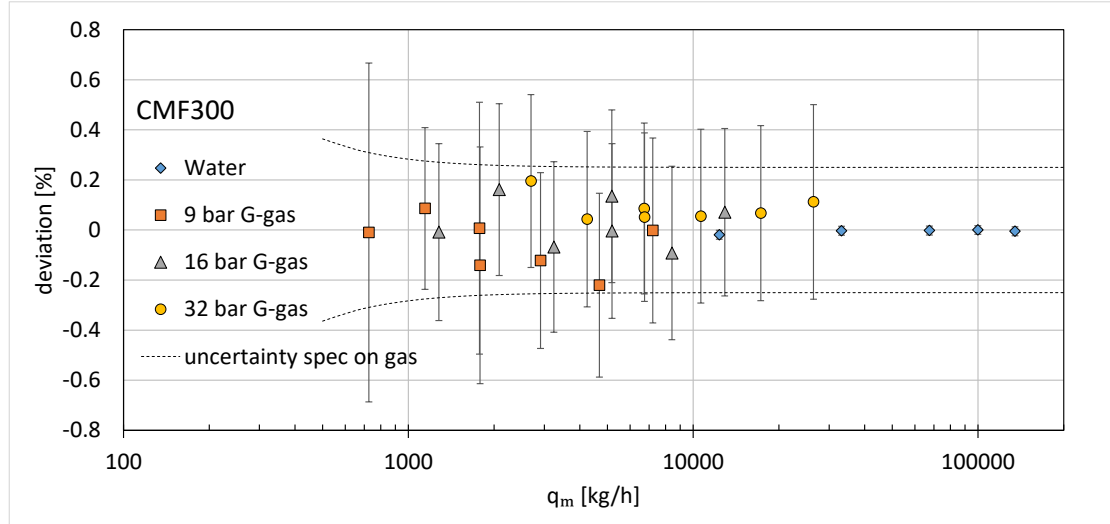


Fig. 6 – Results from the CMF300 checks at 9,16 and 32 bara on Groningen natural gas.

### 3.3 Turbine meters

Two new FMG turbine gasmeters with nominal diameters DN100 and DN150, were first calibrated at PTB in Braunschweig with atmospheric air to determine the parameters of the PTB turbine meter model [4],[5], which has proven to be adequate in scaling across different pressure steps and from air to natural gas. This step was followed by a high-pressure calibration with natural gas at DNV in Groningen. The parameters of the PTB turbine meter model are based on all available calibrations.

The PTB turbine meter model describes the deviation of a turbine gasmeter  $e_{TM}$  as the sum of three contributions. For normal operation flow forces are dominant, resulting in a contribution  $e_{Re}$ . At low speeds the contribution  $e_b$  from the bearing friction becomes important. And for high flow velocities there is a contribution  $e_p$  due to the expansion of the gas flow between the pressure reference point and the temperature measurement downstream of the meter. The deviation of a turbine gasmeter  $e_{TM}$  can now be written as the sum of these three contributions:

$$e_{TM} = e_{Re} + e_b + e_p \quad (5)$$

where

$$e_{Re} = \sum_{j=0}^n a_j [\log(Re/10^6)]^j \quad (6) \quad e_b = \frac{b_0}{\rho Q^2} + \frac{b_1}{\rho Q} \quad (7) \quad e_p = c_p Q^2 \frac{\rho}{p} \quad (8)$$

in which  $b_0$ ,  $b_1$  are empirical coefficients determined in so-called spin tests and jump tests [5],  $c_p$  is an empirical coefficient dependent on the gas composition via the isentropic expansion factor  $\kappa$ ,  $a_j$  are coefficients determined by a least-squares



approximation,  $n$  is the maximum number of coefficients  $a_j$  minus 1, optimised for minimum residue. In practise  $n \leq 4$ . The meter inlet Reynolds number  $Re$  is defined as:

$$Re = \frac{\rho v D}{\eta} = \frac{4\rho Q}{\pi D \eta} \quad (9)$$

Here  $v$  is the average flow velocity,  $D$  the nominal diameter of the meter inlet and  $\eta$  the dynamic viscosity.

After the air calibrations performed at PTB, the system was calibrated at the DNV test facility in Groningen. The calibration was done by installing the full reference skid, including the Coriolis meters at approximately 10D upstream the turbine meters. This installation is different from the installation at PTB where both turbine meters were installed with more than 10D free upstream length. The results of the turbine meters at the three pressures are given in Fig. 7, for the DN100 and DN150, as a function of the Reynolds number, where the error bars indicate the combined facility CMC and meter repeatability.

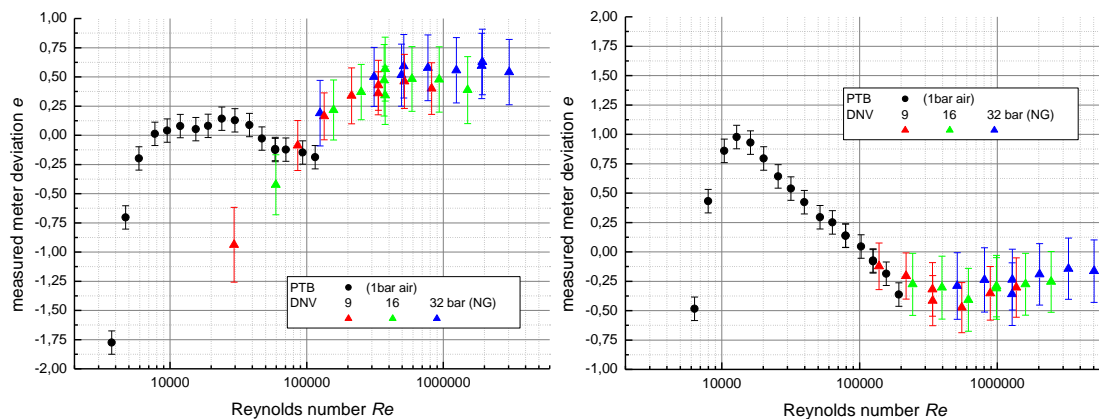


Fig. 7 – Calibration results of the FMG DN100 (TM6) on the left and FMG DN150 (TM7) on the right obtained with atmospheric air and with Groningen gas at 9,16 and 32 bara.

The coefficients resulting from the air and natural gas flow calibrations and the spin and jump tests are summarised in Table 4.

**Table 4 – Values of the coefficients of the turbine gasmeter model for turbine meters TM6 and TM7**

Meter	$b_0$ [kg m <sup>3</sup> /s <sup>2</sup> ]	$b_1$ [kg/s]	$c_{p,air}$ [m <sup>-4</sup> ]	$c_{p,NG}$ [m <sup>-4</sup> ]
TM6 (DN100)	-6.54E-05	-0.02492	-1600000	-1600000
TM7 (DN150)	-4.62E-04	-0.04487	-180000	-180000

Meter	$a_0$ [-]	$a_1$ [-]	$a_2$ [-]	$a_3$ [-]	$a_4$ [-]
TM6 (DN100)	0.50900	0.41715	-0.34513	-0.41518	0.56025
TM7 (DN150)	-0.24521	-0.50144	1.0605	0.19335	-0.55424

## 4 DATA PROCESSING AND CALIBRATION UNCERTAINTY

### 4.1 Traceability

The traceability chains of the meters under test used in the JIP are graphically displayed in Fig. 8. Each type of reference has its own traceability chain. The nozzles are traceable to the metre both via dimensional measurements (throat diameter and curvature) and the PTB air flow facility. The Coriolis meters are traceable via Emerson's test facility in Ede (NL) to the kilogram and the turbine gasmeters are traceable via DNV and FORCE. The calibrations of the turbine gasmeters with atmospheric air are primarily used to evaluate the parameters of the bearing friction. For this reason, this connection is represented by a dashed line. Also the checks of the Coriolis meters at DNV's high-pressure gas flow facility are not considered part of their traceability.

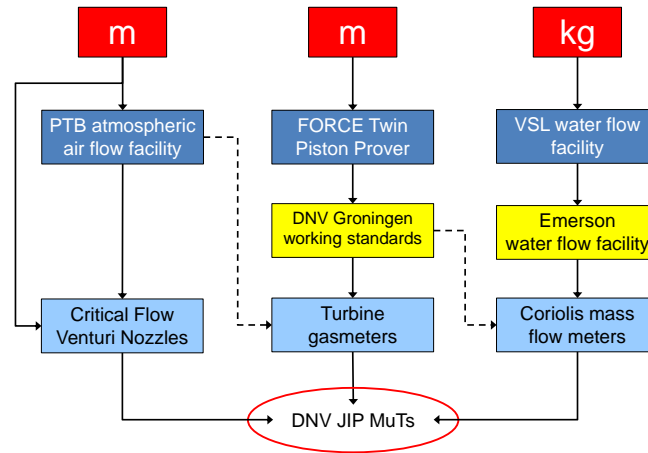


Fig. 8 – Traceability chain of the JIP references (light blue), which are used to calibrate the meters under test. The red rectangles indicate the connection with the base SI-unit, the dark blue rectangles are the primary facilities, and the yellow rectangles represent the working standard to calibrate the instruments. The dashed lines are either checks or evaluation of model parameters.

Equations (10), (11) and (12) show the calculation of the mass flow  $q_m$  for turbine gasmeters, Coriolis mass meters and sonic nozzles, respectively.

$$q_{TM} = \frac{\rho Q_{TM}}{1 + e_{TM}} = \frac{p M}{Z R_u T} \cdot \frac{Q_{TM}}{1 + e_{TM}} \quad (10)$$

$$q_{CMF} = q_{g,CMF}^c \quad (11)$$

$$q_{SN} = A_{throat} C_D c^* \frac{p_0 \sqrt{M}}{\sqrt{R_u T_0}} \quad (12)$$

In equations (10)-(12)  $p$  is the pressure,  $M$  the molar mass,  $Z$  the real gas factor,  $R_u$  the universal gas constant,  $T$  the absolute temperature,  $Q_{TM}$  the volume flowrate indicated by the turbine gasmeter,  $e_{TM}$  is the deviation or error of the turbine meter calculated from equations (5)-(8),  $q_{g,CMF}^c$  the compensated mass flowrate calculated from equations (2)-(4),  $A_{throat}$  is the nozzle throat cross-sectional area,  $C_D$  the discharge factor,  $c^*$  the critical flow factor, and the 0 in  $p$  and  $T$  refers to stagnation

conditions. Please observe the molar mass  $M$  is identical in both equation (10) and (12). This introduces a correlation that will be taken care of later.

## 4.2 Mass flow uncertainties

### 4.2.1 Nozzles

For the sonic nozzles the uncertainty analysis is based on equation (12). In Table 5 the expanded percentual uncertainty of the nozzle mass flow is shown for all input parameters. Due to the 3  $\mu\text{m}$  manufacturing uncertainty of the nozzle diameter the uncertainty (0.18%) of the smallest nozzle is higher than the uncertainty of the largest nozzle (0.13%).

**Table 5 – Uncertainty ( $k = 2$ ) of the nozzle mass flow.**

Quantity	Sensitivity	Uncertainty [%]
Discharge coefficient $C_D$	1	0.10
Critical flow factor $c^*$	1	0.05
Stagnation pressure $p_0$	1	0.04
Stagnation temperature $T_0$	0.5	0.04
Molar mass $M$	0.5	0.10
Universal gas constant $R_u$	0.5	0.01
Throat cross section $A_{throat}$ (based on 3 $\mu\text{m}$ diameter uncertainty)	1	0.12 (D5) ... 0.02 (D27)
<b>Overall uncertainty in <math>q_m</math></b>		<b>0.13 ... 0.18</b>

### 4.2.2 Coriolis meters

The uncertainty of the Coriolis mass flow rate consists of the base uncertainty of 0.25% for high-pressure gas application and the zero-stability expressed by the following formulas

$$U_{\text{CMF200}}^2 = \left( \frac{K \cdot 1.3}{q_{\text{CMF200}}} \right)^2 + 0.0025^2 \quad (13) \quad U_{\text{CMF300}}^2 = \left( \frac{K \cdot 4.4}{q_{\text{CMF300}}} \right)^2 + 0.0025^2 \quad (14)$$

where  $q_{\text{CMFxxx}}$  is the actual mass flowrate [kg/h] through the Coriolis meter. As the zero stability during the experiments appeared much better than indicated on the data sheet of the Coriolis meters [8], an empirical constant  $K = 0.3$  was introduced. Taking the square root and multiplying with 100 gives the percent value, which is 0,25%.

### 4.2.3 Turbine gasmeters

For the turbine gasmeters the uncertainty analysis is based on equation (10). The result is presented in Table 6. During the experiments a shift of the smaller turbine meter of 0.2% was observed. The correction was made by changing the  $a_0$  coefficient at the additional expense of 0.02% uncertainty. During the experiments the uncertainty of the TM6 due to reproducibility needed to be enlarged to 0.15%. For this reason, the TM6 has a little higher uncertainty than the TM7.

**Table 6 – Uncertainty ( $k = 2$ ) of the mass flow through the turbine meter.**

Quantity	Uncertainty / %	
	TM6	TM7
Pressure $p$	0.04	
Temperature $T$	0.03	
Molar mass $M$	0.10	
Universal gas constant $R_u$	0.01	
Real gas factor $Z$	0.10	
Volume flowrate $Q_{TM}$	$< 10^{-5}$	
Reproducibility of deviation	0.15	0.05
Traceability of deviation $e_{TM}$	0.15	
Bearing friction	20% of applied correction	
Interpolation shift	0.02	-
<b>Overall uncertainty in <math>q_m</math></b>	<b>0.26</b>	<b>0.22</b>

#### 4.2.4 Flowrate dependent uncertainties

The uncertainties of the mass flows are dependent on the instrument used and the flowrate. Fig. 9 shows the expanded uncertainties of both turbine meters (red dots), both Coriolis meters (green dots), all five nozzles (blue dots), and the common reference value (black dots). For the turbine meters there is an influence of the curve fit which leads to an uncertainty increase at both ends of the fitted curve. The difference in uncertainty between the smaller and the bigger turbine meter is clearly visible. The CMM uncertainties are the result of equations (13) and (14).

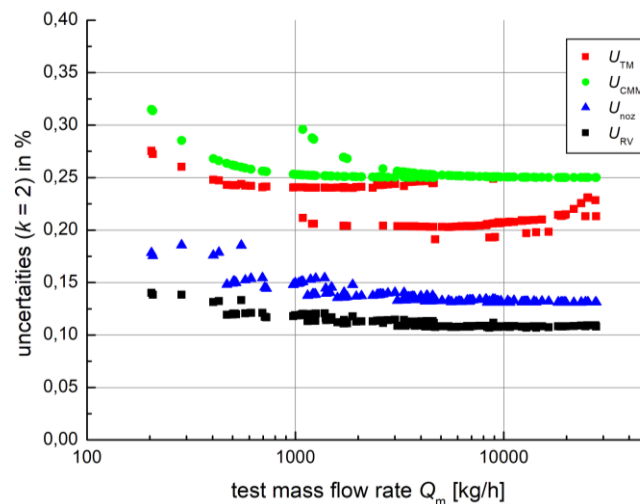


Fig. 9 – Flow-dependent expanded uncertainties of the reference system. The red dots represent the turbine meters, the green dots the mass flowmeters, the blue dots the sonic nozzles and the black dots represent the common reference value.

### 4.3 $E_n$ values

#### 4.3.1 Without correlation

As all types of reference instruments have independent traceability, a common reference value for the mass flow can be established in the same way as in

international intercomparisons [11], and which is done for the harmonised cubic metre [12]. The common reference value of the mass flowrate  $q_{\text{CRV}}$  is

$$q_{\text{CRV}} = \frac{1}{W} [w_{\text{TM}} q_{\text{TM}} + w_{\text{CMF}} q_{\text{CMF}} + w_{\text{SN}} q_{\text{SN}}] \quad (15)$$

where  $w_{\text{xx}}$  is the weighing factor that equals the inverse of the squared uncertainties

$$w_{\text{TM}} = \frac{1}{u_{q,\text{TM}}^2} \quad w_{\text{CMF}} = \frac{1}{u_{q,\text{CMF}}^2} \quad w_{\text{SN}} = \frac{1}{u_{q,\text{SN}}^2} \quad (16)$$

where  $u_{q,\text{xx}}$  is the standard uncertainty ( $k = 1$ ) of mass flow measured by the respective instrument, which is determined in conformity with the GUM [13].  $W$  is the sum of the weighing factors.

$$W = w_{\text{TM}} + w_{\text{CMF}} + w_{\text{SN}} \quad (17)$$

The (expanded,  $k = 2$ ) uncertainty of the common reference value of the mass flow is

$$U_{q,\text{CRV}} = k/\sqrt{W} \quad (18)$$

The value of  $U_{q,\text{CRV}}$  is 0.12%, which is much better than each of the references would achieve by itself. The last step of is the determination of the normalised difference  $E_n$ , also called degree of equivalence. This quantity is defined as the difference between the mass flow of the instrument  $q_{\text{xx}}$  and the common reference flow  $q_{\text{CRV}}$  divided by the expanded uncertainty ( $k = 2$ ) of this difference. For the turbine gasmeter  $E_n$  is

$$E_{n,\text{TM}} = \frac{q_{\text{TM}} - q_{\text{CRV}}}{k \sqrt{u_{q,\text{TM}}^2 - u_{q,\text{CRV}}^2}} \quad (19)$$

For the other instruments identical equations are used. If  $|E_n| \leq 1$  the difference is not significant with 95% confidence level, which means that five  $E_n$  values out of hundred may be higher than 1 or smaller than -1.

#### 4.3.2 With correlation

As mentioned before the mass flowrates from the turbine gasmeters and sonic nozzles are correlated via the molar mass  $M$ . Now the calculations are reproduced via matrix calculations, in which the correlation is implemented. The variance-covariance matrix  $\mathbf{V}_q$  of the input values is

$$\mathbf{V}_q = \begin{pmatrix} u_{\text{TM}}^2 & \text{cov}_{\text{TM,SN}} & 0 \\ \text{cov}_{\text{TM,SN}} & u_{\text{SN}}^2 & 0 \\ 0 & 0 & u_{\text{CMF}}^2 \end{pmatrix} \quad (20)$$

where  $\text{cov}_{\text{TM,SN}}$  is the covariance between indication of the turbines and the sonic nozzles introduced by the molar mass. The uncertainty of the molar mass  $u_M$  is part of the uncertainty budget of the turbine meter with sensitivity  $c_{M,\text{TM}} = 1$  and of the sonic nozzle with sensitivity  $c_{M,\text{SN}} = 0.5$  (see also equations (10) and (12)). Hence, the covariance between turbine and sonic nozzle is:

$$\text{cov}_{\text{TM,SN}} = c_{M,\text{TM}} c_{M,\text{SN}} u_M^2 = 0.5 u_M^2 \quad (21)$$

This results into the weighing matrix

$$\mathbf{W}_q = \mathbf{V}_q^{-1} = \begin{pmatrix} w_{TM}^2 & w_{C_{TM,SN}} & 0 \\ w_{C_{TM,SN}} & w_{SN}^2 & 0 \\ 0 & 0 & w_{CMF}^2 \end{pmatrix} \quad (22)$$

Applying the algebraic rules of matrix calculation for the propagation of uncertainties in linear models we get for the reference value and its uncertainty

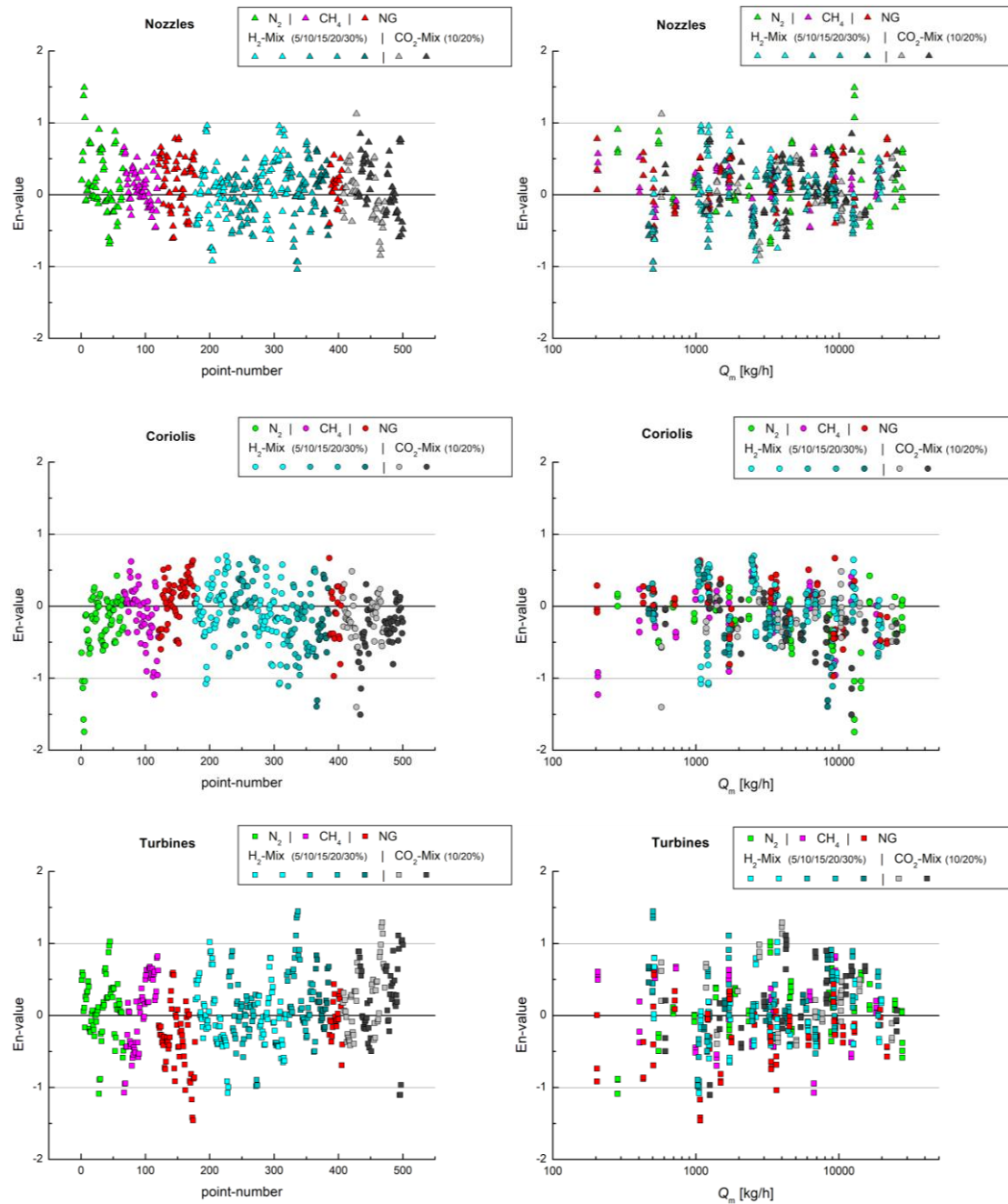


Fig. 10 –  $E_n$  values of the nozzles (top row), Coriolis meters (middle row) and turbine gasmeters (bottom row). The left column shows the  $E_n$  for each measurement point number, the right column shows  $E_n$  versus the mass flowrate  $q_{CRV}$  [kg/h], which is logarithmically displayed.

$$q_{\text{CRV}} = \frac{1}{W} \left[ (w_{\text{TM}} + w c_{\text{TM,SN}}) q_{\text{TM}} + w_{\text{CMF}} q_{\text{CMF}} + (w_{\text{SN}} + w c_{\text{TM,SN}}) q_{\text{SN}} \right] \quad (23)$$

$$W = w_{\text{TM}} + w_{\text{CMF}} + w_{\text{SN}} + 2 w c_{\text{TM,SN}} \quad (24)$$

$$U_{q,\text{CRV}} = k/\sqrt{W} \quad (25)$$

The calculation of the  $E_n$  values remains identical to equation (19)

The  $E_n$  values of the correlation-based analysis are depicted in Fig. 10. The left column shows the  $E_n$  based on equation (19), as a function of the test-point number. In the right-hand column  $E_n$  is shown versus the logarithmic mass flowrate. The top row shows the results for the sonic nozzles, the middle row for the Coriolis meters and the bottom row for the turbine gasmeters. In Fig. 10 only the data are shown where records are available of all three instrument types. As expected, there is only a limited number of data points that exceed  $|E_n| = 1$ . The corresponding numbers and percentages are shown in Table 7. Less than 5% of the  $|E_n|$  are greater than 1.

**Table 7 – Number (#) and percentage (%) of values for  $|E_n|$  categories up to 0.5, between 0.5 and 1, and over 1.**

$E_n$	Turbine gasmeters		Coriolis meters		Sonic nozzles	
	#	%	#	%	#	%
$0 \leq  E_n  \leq 0.5$	367	73%	397	79%	399	80%
$0.5 <  E_n  \leq 1$	112	22%	87	17%	96	19%
$ E_n  > 1$	21	4%	16	3%	5	1%
Total	500	100%	500	100%	500	100%

## 5 RESULTS AND DISCUSSION

All sonic nozzles, accurately manufactured according the ISO9300 specification, can be described with one equation for the discharge factor  $C_D$  using one free parameter. The results of all check measurements with natural gas at pignar and with 16 bar compressed air are located within a band of  $\pm 0.1\%$ . The mass flow uncertainty of the nozzles ranges between 0.13% and 0.18%, depending on the size of the nozzle.

Both Coriolis meters are used far below their calibrated minimum water flowrates of 4431 kg/h and 12342 kg/h. The checks of the CMF300 on natural gas range down to 600 kg/h. For the CMF200 there are no verification data. The lowest flowrate during the experiments was 200 kg/h. Despite the Coriolis meters are used far below the limit of the water calibration, the measurement results are consistent with the other measurement technologies. However, a water calibration down to 200 kg/h will keep the traceability chain of the Coriolis meters independent of the other traceability chains. The zero-stability observed during the experiments appeared to be much better than listed in the product specifications [8]. For this reason the uncertainty contribution due to zero stability could be reduced to 30% of the specification. See equations (13) and (14).

During the measurements, the smallest turbine meter showed a shift of 0,2%, which was corrected. After the correction consistent results were obtained. A

recalibration on both air and natural gas will clarify if the meter has shifted, which is to be expected for a very new gasmeter.

The consistency of the comparison of nozzles, turbine and Coriolis meters demonstrates that the uncertainties of the mass flowrates are realistic. The normalised deviations  $|E_n|$  are generally smaller than 1. Only 4% of the turbine meter values, 3% of the Coriolis values and 1% of the sonic nozzle values are exceeding  $|E_n| = 1$ .

## 6 CONCLUSIONS AND OUTLOOK

For the first time in the metrological history of high-pressure gas-flow measurements, a reference flow system was used, consisting of sonic nozzles, turbine meters and Coriolis meters, that are operated simultaneously. In this way the operational uncertainty is lower than the uncertainty that is achievable by each of the technologies separately. This reference system is also the result of more than 20 years of PTB research on the discharge coefficient of sonic nozzles and the development of the PTB turbine model. The result of these efforts is that the performance of both nozzles and turbine meters can be scaled independent of pressure, for a variety of gases, including hydrogen-enriched natural gas.

As the three instrument types have completely independent traceability chains, the measurement uncertainty of the average flowrate can be calculated in the same way as the common reference value in intercomparisons. The resulting uncertainty of 0.12% meets the best available in the high-pressure calibration market.

The reference system works well as was demonstrated by the uncertainty analysis. The normalised deviations  $|E_n|$  are generally smaller than 1. Only 4% of the turbine meter values, 3% of the Coriolis values and 1% of the sonic nozzle values are exceeding  $|E_n| = 1$ , which is good considering the 95% confidence of the  $E_n$  criterion. This indicates that the uncertainties attributed to the mass flowrate are realistic.

In the near future the turbine gasmeters will be checked for stability on both air and natural gas. Now these new meters are in use, the bearing friction is expected to reduce, which will lead to a shift of the curve in the lower operating range of the meter. Based on operational experiences, the turbine meters will be stable after this initial phase. The Coriolis meters will also be recalibrated with natural gas, preferably down to 200 kg/h, if possible, also with water. The common reference values are not expected to change much, as the sonic nozzles do not change, and their uncertainty is the lowest of all references. As this is the first time the designed reference system is used in practise, it will be useful to repeat the experiments. One point that can easily be improved, is to allow more time for the loop to stabilise, which will further improve the results.

## 7 SUMMARY

For the first time in the history of high-pressure gas flow measurements a reference system has been realised that consists of three metering technologies: turbine gasmeters, Coriolis meters and sonic nozzles. The system is designed for the calibration of flowmeters using different gases and gas mixtures. The models for the discharge coefficients and the turbine gasmeters compensate the different thermodynamical properties of the gases and gas mixtures. For this reason, the



system works independently of pressure and gas composition. The mass flowrate of the reference system is the uncertainty-weighted average of all three meter types. As the three instrument types have completely independent traceability chains, the measurement uncertainty of the average flowrate can be calculated in the same way as the common reference value in intercomparisons. The resulting uncertainty of 0.12% meets the best available CMCs in the high-pressure calibration market.

## 8 NOTATION

Abbreviations		$Q$	volume flowrate	[m <sup>3</sup> /h]
MuT	Meter under Test	$q_m$	mass flowrate	[kg/s]
CCS	carbon capture and storage	$R_c$	nozzle curvature radius (normalised with $d_{throat}$ )	[-]
CMC	calibration measurement capability	$Re$	Reynolds number	[-]
CMF	Coriolis mass flowmeter	$R_u$	universal gas constant	[J·K <sup>-1</sup> ·mol <sup>-1</sup> ]
CMM	Coriolis mass flow meter	$r$	radius	[m]
JIP	Joint Industry Project	$r_n$	radius, normalised (normalised with $d_{throat}$ )	[-]
SN	Critical Flow Venturi Nozzle or Sonic Nozzle	$T_0$	stagnation temperature	[K]
TM	Turbine gasmeter	$t$	time	[s]
Latin symbols		$U$	expanded uncertainty	
$A$	cross-sectional area	$u$	standard uncertainty	
$a_j$	coefficient turbine gasmeter	$W$	sum of weighing factors	
$b_0$	coefficient turbine gasmeter	$w$	weighing factor	
		$z$	axial position in the nozzle	[m]
$b_1$	coefficient turbine gasmeter	Greek symbols		
$c_p$	coefficient turbine gasmeter (gas composition dependent)	$\kappa$	isentropic exponent	[-]
		$\rho$	mass density	[kg/m <sup>3</sup> ]
$C_D$	discharge coefficient	$\Omega_c$	curvature = $R_c^{-1}$	[-]
$C^*$	critical flow factor	Index		
$D$	Nominal internal diameter of the turbine gasmeter	0	stagnation conditions	
		CMF	Coriolis meter	
$d$	diameter	$m$	mass	
$e$	deviation or error	MuT	meter under test	
$f$	correction factor	Ref	reference	
$k$	coverage factor	SN	sonic nozzle	
$M$	molar mass	TM	turbine gasmeter	
$m$	mass	throat	at throat conditions	
$n$	exponent			
$p_0$	stagnation pressure			
$p_c$	CMM calibration pressure			

## 9 REFERENCES

- [1] <https://www.dnv.com/oilgas/joint-industry-projects/2019-jip-initiations/Influence-of-non-conventional-gases-on-gas-flow-meters.html>
- [2] Dennis van Putten, Henk Riezebos, Mohammed Al Saleem (2021): Assessment of renewable gases influence on gas flow meters, 39<sup>th</sup> International North Sea Flow Measurement Workshop, 26 – 29 October 2021, to be published.
- [3] Bodo Mickan, Jos van der Grinten and Thomas Kappes (2020): [Primary and secondary flow standards for a wide variety of gas compositions – a solid base for reliable traceability facing the energy transition](#), 38<sup>th</sup> International North Sea Flow Measurement Workshop, 26 – 29 October 2020.

- [4] Jos G.M. van der Grinten, Arnthor Gunnarsson, Mijndert van der Beek and Bodo Mickan (2019): [An intercomparison between primary high-pressure gas flow standards with sub-permille uncertainties](#), 37<sup>th</sup> International North Sea Flow Measurement Workshop, Tønsberg, Norway, 22 - 24 October 2019, Reprinted in Cal Lab: The International Journal of Metrology, [vol 27\(4\), 2020](#), pp 28-35.
- [5] Böckler, H.-B.: *Messrichtigkeit von mechanischen Gasmessgeräten bei Verwendung von unterschiedlichen Gasbeschaffenheiten*, Dissertation, Universität Duisburg-Essen, 2019, ISBN 978-3-95606-493-7
- [6] International Standards Organization: *Measurement of Gas Flow by Means of Critical Flow Venturi Nozzles*, ISO 9300:2005(E)
- [7] Aart Pruysen: *Renewable gases Micro Motion Coriolis – Diagnosis and suggestions*, presentation for DNV JIP, 1 March 2021.
- [8] Emerson: [Micro Motion™ ELITE™ Coriolis Flow and Density Meters](#), Product Data Sheet PS-00374, Rev AK, January 2020.
- [9] J. Hemp and J. Kutin: [Theory of errors in Coriolis flowmeter readings due to compressibility of the fluid being metered](#), Flow Measurement and Instrumentation 17 (2006) 359–369.
- [10] AGA10 *Speed of Sound in Natural Gas and Other Related Hydrocarbon Gases*, AGA Transmission Measurement Committee Report No. 10, Catalog No. XQ0310.
- [11] Cox, M. G. [The evaluation of key comparison data](#), Metrologia, **39**(6), pp 589-595, 2002.
- [12] Jos van der Grinten, Henri Foulon, Arnthor Gunnarsson, Bodo Mickan (2018): [Reducing measurement uncertainties of high-pressure gas flow calibrations by using reference values based on multiple independent traceability chains](#), Technisches Messen, Vol. 85(12), pp 754-763, <https://doi.org/10.1515/teme-2018-0019>
- [13] JCGM 100 (2008): [Evaluation of measurement data - Guide to the expression of uncertainty in measurement](#), Guide JCGM 100.